Supplement figures

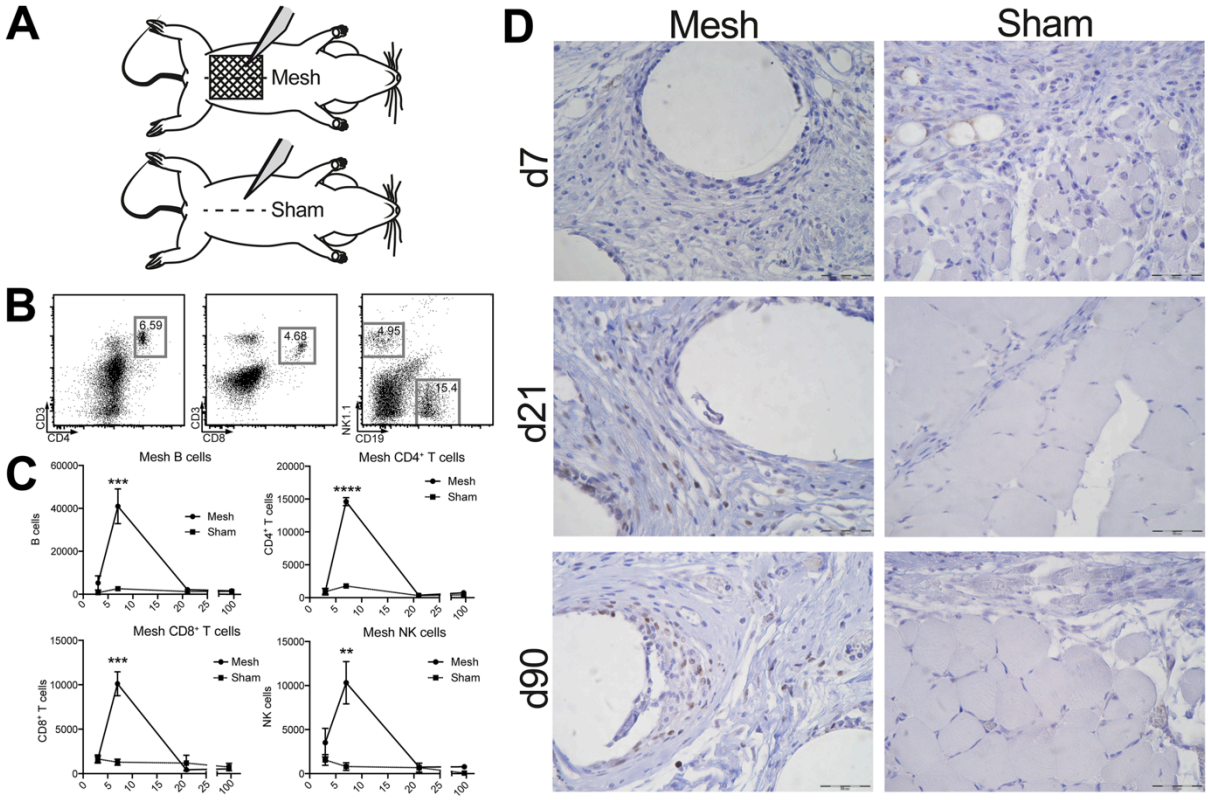

Supp. Figure 1: **A** Description of the murine model of abdominal mesh implantation. Mice were surgically transplanted with polypropylene (PP) meshes by surgical exposition of the abdominal wall and subcutaneous instillation of mesh segments with a size of approximately 2cm^2. For explantation, mice were sacrificed, and the mesh was explanted including the underlying muscular layer and abdominal fascia. Sham surgery was performed in a similar manner despite the deposition of the PP mesh. Characterization of lymphoid cellular infiltrates in murine mesh samples at early and late stages following implantation. **B** Exemplary gating to characterize lymphoid cell populations in the foreign body granulomas. **C** Quantification of leukocyte subpopulations of the populations shown in B. **D** Lymphocyte staining with PAX5 antibody in murine mesh explants. Exemplary results are shown in the dot plots, statistical analysis was performed from 4 animals per group in two independent sets of experiments. Student's T test: *P<0.05; **P<0.01; ***P<0.001, ****P<0.0001. Error bars represent mean ± SD.

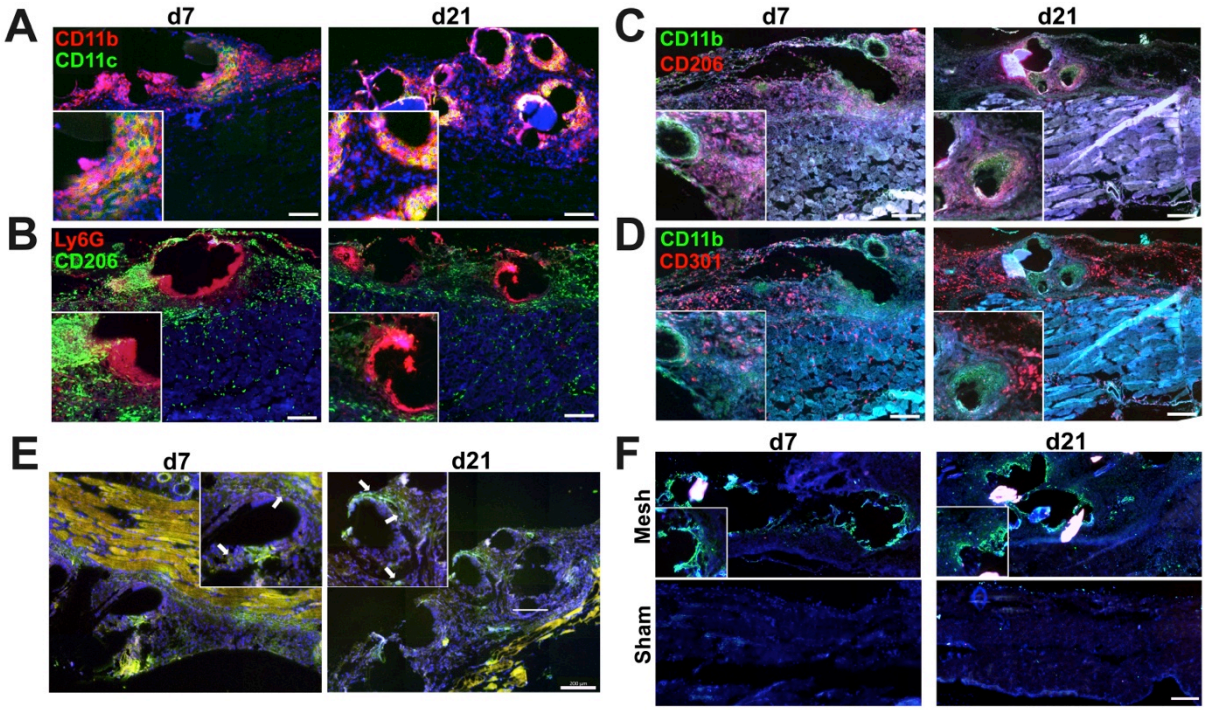

Supp. Figure 2: *Multicolor immunofluorescence staining from mesh explants and sham operated animals.* Costainings were perfomed for **A** CD11b & CD11c, **B** CD11b & CD206, **C** Ly6G & CD206 and **D** CD11b & CD301. Scale bar 500µm. **E** Nlrp3 fluorescence in situ hybridization (FISH) staining. Cryosections derived from tissue explants from mice subjected to abdominal mesh implantation were stained for Nlrp3 gene expression using a directly coupled FISH probe tagged with Alexa488 (green). Hybridization was performed overnight, nuclei were stained with Hoechst33258 (blue). Inlay images show magnified granulomatous structures around mesh fibers. Scale bar 200µm. **F** TUNEL staining of mesh associated foreign body infiltrates. $TUNEL^{+}$ cells were stained in green, nuclei were stained with Hoechst33258 (blue). Scale bar 200µm. Exemplary results are shown in the pictures, results were verified in at least 3 animals per group from two independent sets of experiments.

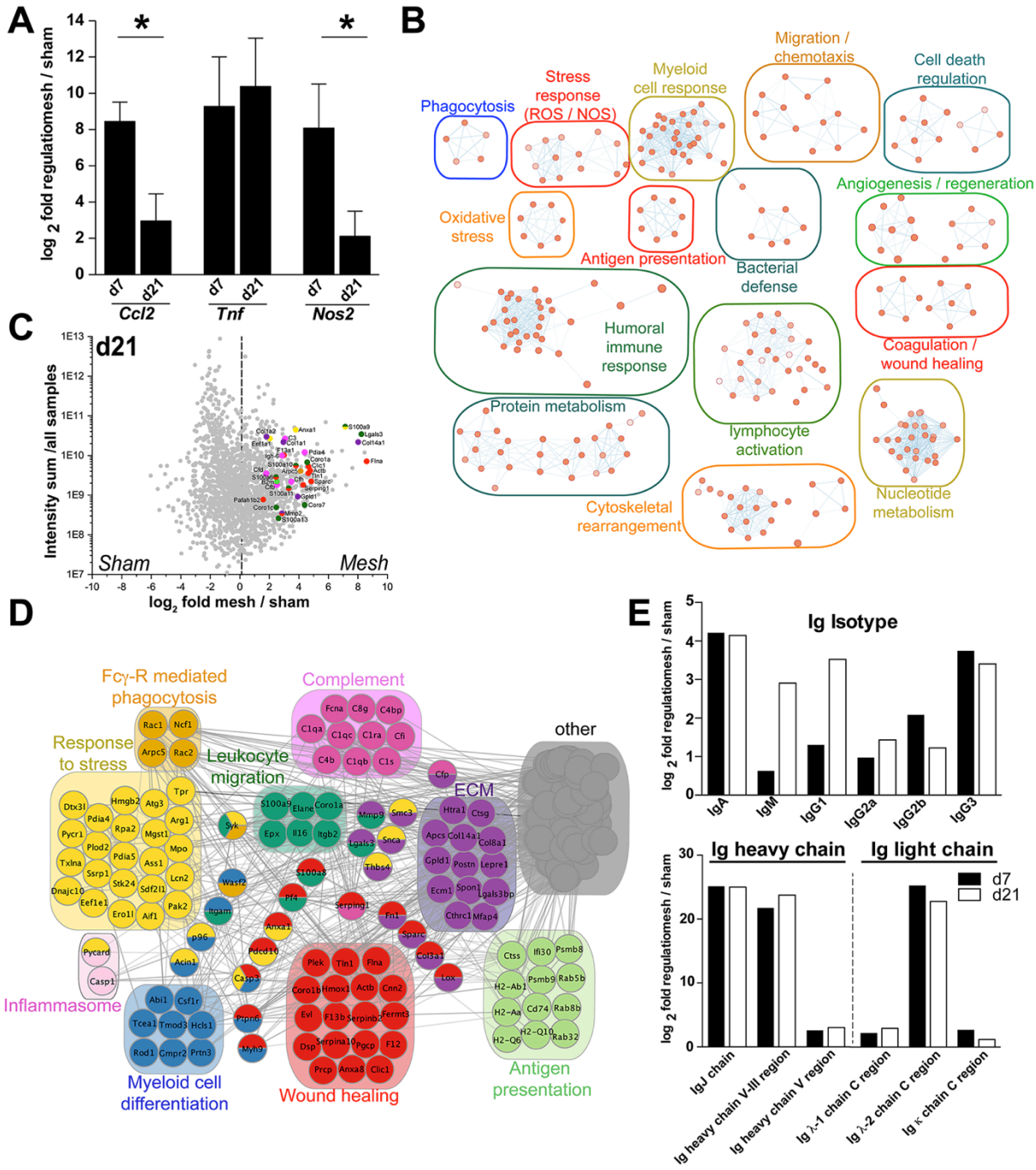

Supp. Figure 3: *Characterization of inflammatory gene expression and protein deposition following mesh implantation*. **A** Exemplary quantitative real time RT-PCR of functionally relevant genes for macrophage recruitment and activation. Nanostring gene profiling was validated by quantitative RT-PCR for expression of *Ccl2*, *Tnf* and *Nos2*. Expression was normalized against corresponding sham operated control animals. **B** Protein mass spectrometry of mesh samples at d21. BinGO cluster network analysis of proteins associated with inflammatory GO pathways isolated from mesh-associated tissue. **C** Scatter plot displaying weighted protein expression of mesh and sham isolated tissue. Total protein counts of all samples (sum) were plotted as Y-axis, weighted protein expression was displayed as log2-fold expression ratio. Signature proteins of GO pathways described in D were highlighted in the according colors. **D** String protein interaction network analysis. Proteins expressed with a log2-fold ratio of > 4 in mesh vs sham samples at d21 were filtered for generalized pathways relevant for inflammation, immune system activation and wound healing. Relevant protein networks are shown. **E** Mass spectrometry based quantification of immunoglobulin depositions in mesh-associated tissue at d7 and 21. Antibodies were characterized regarding their Ig isotype according to the abundance of the according heavy chain (top). Ig deposition was further confirmed by analyzing various heavy and light chain peptide fragements (bottom). Protein ratios were calculated against the according sham operated tissue explants (d7 and d21). Student's T test: *P<0.05; **P<0.01; ***P<0.001, ****P<0.0001. Error bars represent mean ± SD.

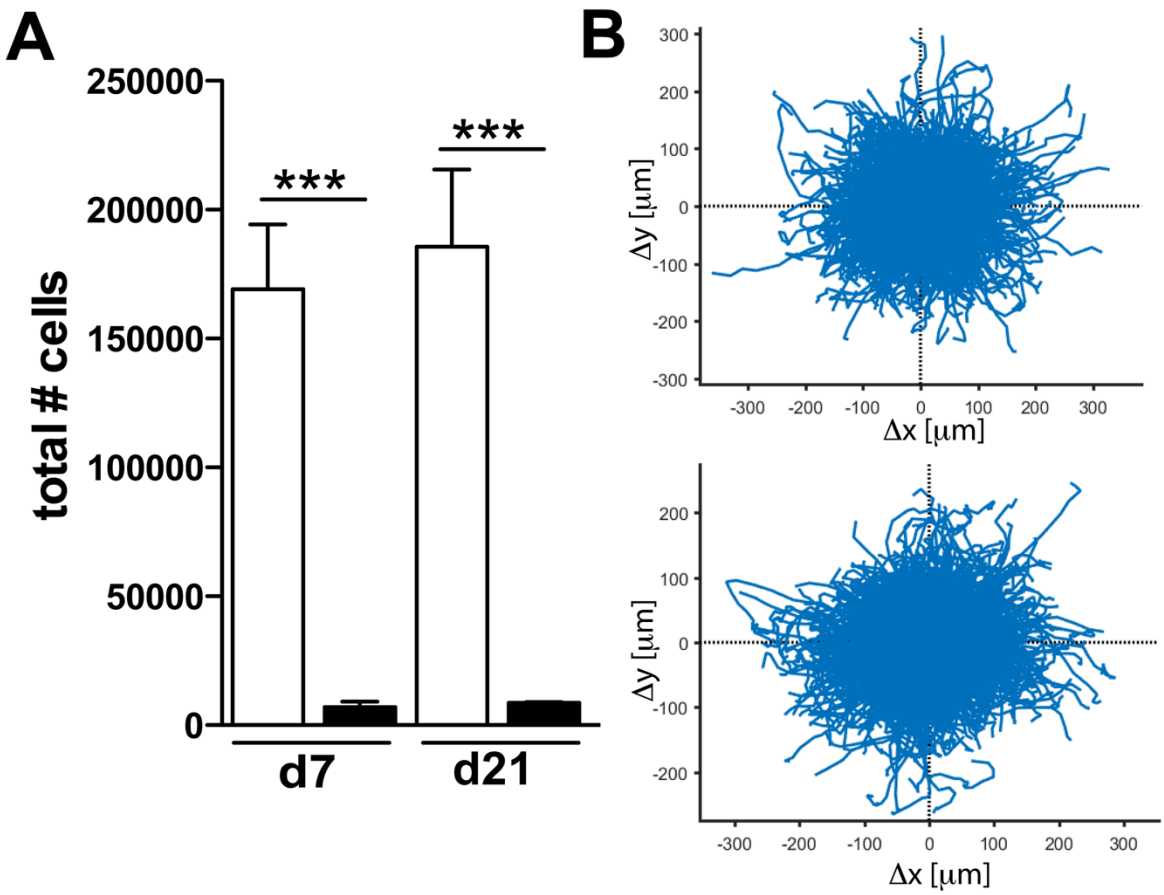

Supp. Figure 4: *Quantification and tracking of CCR2.gfp and Ccr2$^{-/-}$.gfp cells following mesh implantation at d7 and d21.* **A** Flow cytometric assessement of GFP^{+} cells isolated from mesh surrounding tissue after 7 and 21 days. Total cells were counted from tissue segments with a size of 1cm^{2}. **B** Summary plot of cellular migration tracks of GFP^{+} cells in CCR2.gfp mice. Tracks were graphically displayed using a common point of origin to assess cellular motility 7 days (top) and 21 days (bottom) following mesh implantation. Student's T test: *P<0.05; **P<0.01; ***P<0.001, ****P<0.0001. Error bars represent mean ± SD.

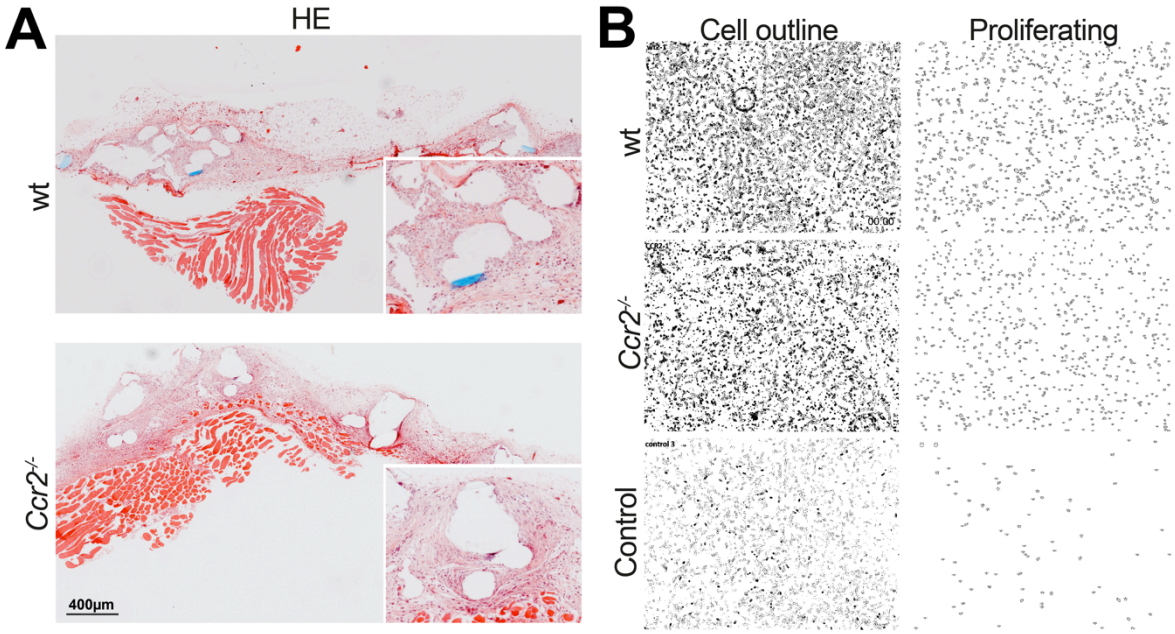

Supp. Figure 5: *Comparison of FBR and fibroblast activation between wt and Ccr2$^{-/-}$ mice.* **A** Histological assessment of mesh associated cellular infiltration by H&E staining. Inlay pictures magnify inflammatory infiltrates. **B** Exemplary binary images derived from phase contrast light microscopy used for quantification of fibroblast proliferation described in Fig. 8. Left column: binary image; right column: outlines of proliferating cells. For statistical analysis, 4 independent fields of view were imaged for each condition.